Letter

Measurement of Born cross section of $e^+e^- \to \Sigma^0\bar{\Sigma}^0$ at $\sqrt{s} = 3.50$–4.95 GeV

M. Ablikim *et al.*[*]

(BESIII Collaboration)

Using e^+e^- collision data collected with the BESIII detector at the BEPCII collider at 32 center-of-mass energies from 3.50 to 4.95 GeV, corresponding to an integrated luminosity of 25 fb^{-1}, we measure the Born cross section of the $e^+e^- \to \Sigma^0\bar{\Sigma}^0$ reaction and the effective form factor for the first time. No significant charmonium(-like) state, i.e., $\psi(3770)$, $\psi(4040)$, $\psi(4160)$, $\psi(4230)$, $\psi(4360)$, $\psi(4415)$, or $\psi(4660)$, decaying into the $\Sigma^0\bar{\Sigma}^0$ final state is observed by fitting the $e^+e^- \to \Sigma^0\bar{\Sigma}^0$ dressed cross section. The upper limits for the product of the branching fraction and the electronic partial width at the 90% confidence level are provided for each assumed charmonium(-like) state for the first time. In addition, the ratios of the Born cross section and the effective form factor between the $e^+e^- \to \Sigma^0\bar{\Sigma}^0$ and the $e^+e^- \to \Sigma^+\bar{\Sigma}^-$ reactions are provided, which can be used to validate the prediction of the vector meson dominance model.

The study of the decays of charmonium(-like) states produced in e^+e^- annihilations into baryon pairs is a key element to test quantum chromodynamics (QCD). The potential model [1] predicts six vector charmonium states in the energy region from 3.7 to 4.7 GeV, identified as the $1D$, $3S$, $2D$, $4S$, $3D$, and $5S$ states [2]. In the past decades, an abundance of charmonium vector states has been observed at e^+e^- colliders above the open-charm threshold. Three conventional charmonium states, i.e., $\psi(4040)$, $\psi(4160)$, and $\psi(4415)$ [3], have been observed in open-charm final states; more recently, three nonconventional charmoniumlike states, i.e., $\psi(4230)$, $\psi(4360)$, and $\psi(4660)$, have been observed in hidden-charm final states via initial state radiation (ISR) processes at *BABAR* and Belle [4–12], or by direct production processes at CLEO [13] and BESIII [14–16]. These states cannot be classified as resonances consisting solely of a $c\bar{c}$ quark pair. The overpopulation of structures and the discrepancies between potential model predictions and experimental measurements suggest that some of these structures may be candidates for exotic states. To explain their nature [17], many hypotheses including hybrid states [18], multiquark states [19], and molecular states [20] have been proposed. However, no definitive conclusion has been drawn. References [21,22] suggest that these states are regarded as pure charmonium states if their baryonic decays can be observed. This situation indicates the imperfect knowledge

of the strong interaction, particularly in its nonperturbative aspects. For a better understanding, more experimental information is desired, such as from the study of charmonium(-like) states decaying into $B\bar{B}$ pairs, where B stands for a baryon, since they provide clear insights into the underlying interaction mechanisms due to their straightforward topology via three gluons process, one virtual photon process and mixed two gluons and one virtual photon process [23]. However, the studies of the decays of charmonium(-like) states above open-charm threshold into $B\bar{B}$ pairs are sparse. Experimental studies have been performed in this energy region by the BESIII experiment [24–34], and the evidence of only $\psi(3770) \to \Lambda\bar{\Lambda}$ and $\psi(3770) \to \Xi^-\bar{\Xi}^+$ [27,30] processes has been reported, while no significant $B\bar{B}$ decays for other vector charmonium(-like) states have been found.

Additionally, the measurement of the electromagnetic and effective form factors of baryon resonances is important to explore their internal composition and electric charge distribution. According to Ref. [35], the branching fractions of charmonium(-like) states decaying into $B\bar{B}$ are expected to be negligible if the reaction is assumed to be dominated by the nonresonant electromagnetic contribution. However, the BESIII experiment [27,30] reported branching fraction values which are at least 1 order of magnitude larger than this prediction ($\sim 10^{-7}$) based on a scaling from the electronic branching fraction values using Eq. (1) in Ref. [35]. The measurement of the cross section of the $e^+e^- \to \Sigma^0\bar{\Sigma}^0$ reaction at center-of-mass energies above the open-charm threshold offers the opportunity to search for the $B\bar{B}$ charmless decays of the vector charmonium(-like) states. Moreover, as proposed by Refs. [36,37], the measured ratios of the Born cross section and the effective form factor between the $e^+e^- \to \Sigma^0\bar{\Sigma}^0$ process

---

[*]Full author list given at the end of the article.

and its isospin partner $e^+e^- \to \Sigma^+\bar{\Sigma}^-$ are important to validate the predictions based on the vector meson dominance model [38–43].

In this paper, we present the measurements of the Born cross section and the effective form factor for the reaction $e^+e^- \to \Sigma^0\bar{\Sigma}^0$, in the range of c.m. energy ($\sqrt{s}$) from 3.50 to 4.95 GeV using e^+e^- collision data corresponding to a total integrated luminosity of 25 fb^{-1} collected with the BESIII detector [44] at the BEPCII collider [45]. The potential resonances are studied by fitting the dressed cross section of the $e^+e^- \to \Sigma^0\bar{\Sigma}^0$ reaction. The upper limits of products of branching fractions and electronic partial widths at the 90% CL for $\psi(3770)$, $\psi(4040)$, $\psi(4160)$, $\psi(4230)$, $\psi(4360)$, $\psi(4415)$, or $\psi(4660)$ decaying into $\Sigma^0\bar{\Sigma}^0$ are provided. In addition, the ratios of the Born cross section and effective form factor between the $e^+e^- \to \Sigma^+\bar{\Sigma}^-$ and $e^+e^- \to \Sigma^0\bar{\Sigma}^0$ reactions are obtained.

Candidate events of $e^+e^- \to \Sigma^0\bar{\Sigma}^0$ are fully reconstructed, i.e., both the baryon and the antibaryon are reconstructed through the $\Sigma^0 \to \Lambda\gamma$ and $\bar{\Sigma}^0 \to \bar{\Lambda}\gamma$ decays, where $\Lambda \to p\pi^-$ and $\bar{\Lambda} \to \bar{p}\pi^+$. The detection efficiency is determined by Monte Carlo (MC) simulations using a sample of 100,000 events for each c.m. energy point, with a uniform phase space (PHSP) model by the KKMC generator [46] including effects of the beam energy spread and ISR corrections. The Σ^0 and $\bar{\Sigma}^0$ decay chains are simulated with the PHSP model by the EvtGen generator [47,48]. The BESIII geometric description and the detector response are modeled with a Geant4-based software package [49].

Charged tracks are reconstructed in the multilayer drift chamber (MDC) within the angular region $|\cos\theta| < 0.93$, where θ is the polar angle with respect to the z axis in the laboratory system, which is the MDC symmetry axis. At least two positive and two negative charged tracks are required to be reconstructed in the MDC. Particle identification (PID) for charged tracks combines measurements of the energy deposited in the MDC (dE/dx) and the flight time in the TOF to form likelihoods $\mathcal{L}(h)(h = p, K, \pi)$ for each hadron h hypothesis. Tracks are identified as protons when the proton hypothesis has the greatest likelihood ($\mathcal{L}(p) > \mathcal{L}(K)$ and $\mathcal{L}(p) > \mathcal{L}(\pi)$), while charged pions are identified by requiring that $\mathcal{L}(\pi) > \mathcal{L}(p)$ and $\mathcal{L}(\pi) > \mathcal{L}(K)$. Events with at least one proton, one antiproton, one positive pion, and one negative pion are kept for further analyses.

Photons are reconstructed from isolated showers in the electromagnetic calorimeter (EMC). The energy deposited in the nearby TOF counter is included to improve the reconstruction efficiency and energy resolution. The energies of photons are required to be greater than 25 MeV in the EMC barrel region ($|\cos\theta| < 0.8$), and greater than 50 MeV in the EMC end cap ($0.86 < |\cos\theta| < 0.92$). Furthermore, the difference between the EMC time and the event start time is required to be within $0 < t < 700$ ns, to suppress electronic noise and energy deposits unrelated to

the collision events. To eliminate showers from charged tracks, the opening angle between the position of each shower in the EMC and any charged track must be greater than 10 degrees. Events with at least two photons are kept for further analyses.

The $\Lambda(\bar{\Lambda})$ candidates are reconstructed via a secondary vertex fit by looping over the $p\pi^-(\bar{p}\pi^+)$ combinations, where for each candidate the corresponding χ^2 value is required to be less than 500. To suppress background events, the condition $|M_{p\pi^-(\bar{p}\pi^+)} - m_{\Lambda(\bar{\Lambda})}| \le 5$ MeV/c^2 is imposed after optimizing the figure-of-merit (FOM = $\mathcal{S}'/\sqrt{\mathcal{S}' + B}$). Here, $M_{p\pi^-(\bar{p}\pi^+)}$ is the invariant mass of the $p\pi^-(\bar{p}\pi^+)$ combination, $m_{\Lambda(\bar{\Lambda})}$ is the nominal mass of the $\Lambda(\bar{\Lambda})$ baryon from the Particle Data Group (PDG) [50], $\mathcal{S}'$ is the number of signal MC events normalized to the real data, and B is the number of the background events taken from the inclusive MC sample of generic $e^+e^- \to$ hadron events.

Afterward, a four-constraint (4C) kinematic fit is applied to all the $\Lambda\bar{\Lambda}\gamma\gamma$ combinations by ensuring the conservation of energy and momentum. The $\Lambda\bar{\Lambda}\gamma\gamma$ combination with the minimum χ^2_{4C} is retained, with an additional requirement of $\chi^2_{4C} < 100$ to further suppress backgrounds. Among the different combinations of $\Lambda\bar{\Lambda}\gamma_1\gamma_2$, the one with the minimum value of $\Delta M = \sqrt{(M_{\Lambda\gamma_1} - m_{\Sigma^0})^2 + (M_{\bar{\Lambda}\gamma_2} - m_{\bar{\Sigma}^0})^2}$ is chosen to identify $\Sigma^0\bar{\Sigma}^0$ events. Here, $M_{\Lambda\gamma_1(\bar{\Lambda}\gamma_2)}$ is the invariant mass of the $\Lambda\gamma_1(\bar{\Lambda}\gamma_2)$ combination, and $m_{\Sigma^0(\bar{\Sigma}^0)}$ is the nominal mass of the $\Sigma^0(\bar{\Sigma}^0)$ baryon from the PDG [50]. Figure 1 shows the distribution of $M_{\bar{\Lambda}\gamma}$ versus $M_{\Lambda\gamma}$. A clear
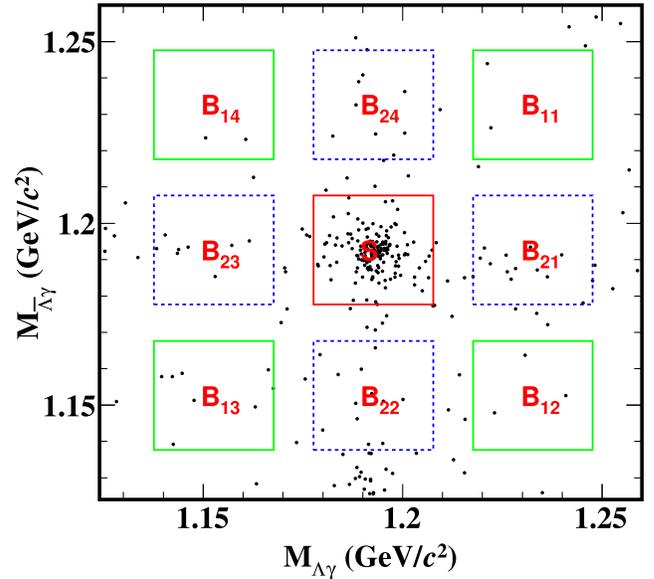

FIG. 1. Distribution of $M_{\bar{\Lambda}\gamma}$ versus $M_{\Lambda\gamma}$ of accepted candidates in data summed over all energies. The red box represents the signal region, and the green boxes and the blue dashed boxes represent the selected sideband regions.

TABLE I.   Definitions of the sideband regions.

	$M_{\gamma\Lambda}$ (GeV/c^2)	$M_{\gamma\bar{\Lambda}}$ (GeV/c^2)
B_{11}	[1.217, 1.247]	[1.217, 1.247]
B_{12}	[1.217, 1.247]	[1.137, 1.167]
B_{13}	[1.137, 1.167]	[1.137, 1.167]
B_{14}	[1.137, 1.167]	[1.217, 1.247]
B_{21}	[1.217, 1.247]	[1.177, 1.207]
B_{22}	[1.177, 1.207]	[1.137, 1.167]
B_{23}	[1.137, 1.167]	[1.177, 1.207]
B_{24}	[1.177, 1.207]	[1.217, 1.247]

event accumulation around the Σ^0 nominal mass can be distinguished. The $\Lambda\gamma(\bar{\Lambda}\gamma)$ combination is required to fall within the mass window $|M_{\Lambda\gamma(\bar{\Lambda}\gamma)} - m_{\Sigma^0(\bar{\Sigma}^0)}| \leq$ 15 MeV/c^2, determined by the FOM optimization.

After applying the event selection criteria, the remaining background events mainly come from the process $e^+e^- \to \Lambda\bar{\Lambda} \to p\bar{p}\pi^+\pi^-$, which has a final state similar to the signal one. To evaluate the background yield in the signal region, eight sideband regions with the same area B_{ij} (where $i = 1, 2$ and $j = 1, 2, 3, 4$) are used for the $M_{\Lambda\gamma}$ and $M_{\bar{\Lambda}\gamma}$ windows as shown in Fig. 1. The sideband regions are defined in Table I. The signal yield N_{obs} for the $e^+e^- \to \Sigma^0\bar{\Sigma}^0$ process at each c.m. energy point is calculated by subtracting the number of background events from the number of events in the signal region, $N_{\text{obs}} = N_{\text{S}} - N_{\text{bkg}}$, where N_{S} is the number of events in the signal region, and N_{bkg} is the number of background events scaled by the sideband region, i.e., $N_{\text{bkg}} = \frac{1}{2}\sum_{i=1}^{4} N_{B_{2i}} - \frac{1}{4}\sum_{j=1}^{4} N_{B_{1j}}$. By using Rolke's method [51], the uncertainty of N_{obs} and its upper limit are calculated. The numerical results are summarized in the Supplemental Material [52].

The Born cross section for the $e^+e^- \to \Sigma^0\bar{\Sigma}^0$ process at a given c.m. energy is calculated by

$$\sigma^B = \frac{N_{\text{obs}}}{\mathcal{L} \cdot (1+\delta) \cdot \frac{1}{|1-\Pi|^2} \cdot \epsilon \cdot \mathcal{B}_{\Sigma^0 \to \Lambda\gamma}^2 \cdot \mathcal{B}_{\Lambda \to p\pi^-}^2}, \quad (1)$$

where $\mathcal{L}$ is the integrated luminosity, $(1+\delta)$ is the ISR correction factor, $\frac{1}{|1-\Pi|^2}$ is the vacuum polarization (VP) correction factor, ϵ is the detection efficiency, $\mathcal{B}_{\Sigma^0 \to \Lambda\gamma}$ and $\mathcal{B}_{\Lambda \to p\pi^-}$ are the corresponding PDG branching fractions [50]. The ISR correction factor is obtained using the QED calculation as described in Ref. [55]. The VP correction factor is calculated according to Ref. [56]. The result of the measured Born cross section for each c.m. energy point is summarized in the Supplemental Material [52]. Note that the efficiencies and ISR correction factors are obtained through an iterative process to accurately measure the Born cross section as proposed in Ref. [57]. Figure 2 shows the line shape of the Born cross section together with the
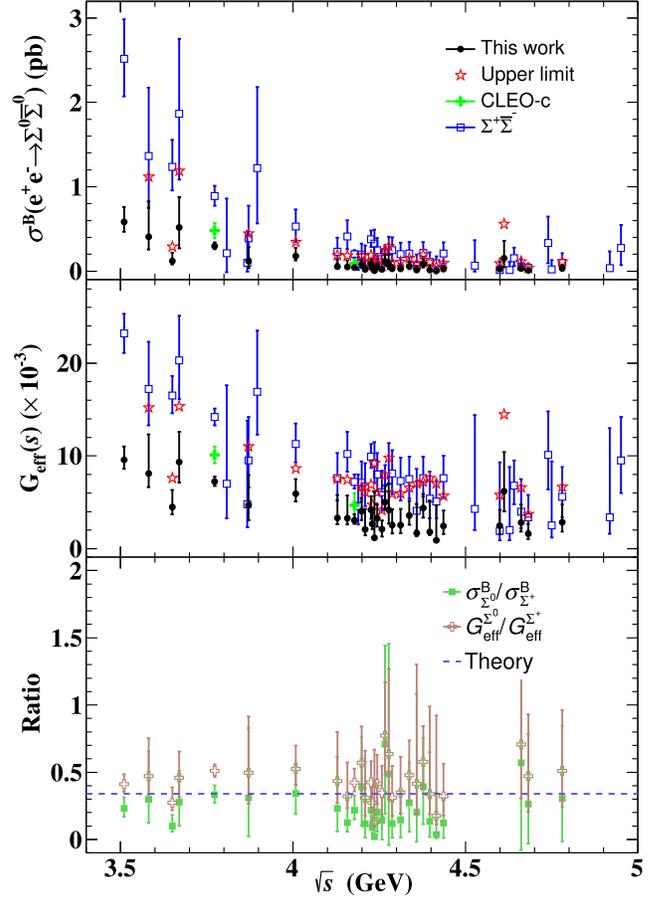

FIG. 2.   Distributions of the Born cross section (upper plots) and the effective form factor (middle plots) as a function of the c.m. energy for the $e^+e^- \to \Sigma^0\bar{\Sigma}^0$ channel, in comparison to the $e^+e^- \to \Sigma^+\bar{\Sigma}^-$ measurements from BESIII [32] and CLEO-c [35]. The bottom plot shows the ratio of the Born cross section and effective form factor between the results of this work and the BESIII results for Σ^+ [32], compared to the theoretical predictions [36].

CLEO-c results at $\sqrt{s} = 3.770$ and 4.160 GeV [35], and the BESIII result for $e^+e^- \to \Sigma^+\bar{\Sigma}^-$ [32].

Under the assumption that the dominant process for the reaction of $e^+e^- \to \Sigma^0\bar{\Sigma}^0$ is the one-photon exchange, the effective form factor $G_{\text{eff}}(s)$ [58] is defined as

$$G_{\text{eff}}(s) = \sqrt{\frac{3s\sigma^B}{4\pi\alpha^2 C\beta\left(\frac{2m_{\Sigma^0}^2}{s} + 1\right)}}, \quad (2)$$

where α is the fine structure constant, $\beta = \sqrt{1 - \frac{1}{\tau}}$ is the velocity with $\tau = \frac{s}{4m_{\Sigma^0}^2}$, m_{Σ^0} is the mass of Σ^0 [50], and the Coulomb factor C [59,60] parametrizes the electromagnetic interaction between the outgoing baryon and antibaryon. For neutral baryons, the Coulomb factor is $C = 1$. Figure 2

shows also a comparison of the effective form factor for the processes $e^+e^- \to \Sigma^0\bar{\Sigma}^0$ and $e^+e^- \to \Sigma^+\bar{\Sigma}^-$ obtained in this work and the previous BESIII result for Σ^+ [32], together with the CLEO-c result for Σ^0 [35].

Systematic uncertainties on the measurement of the Born cross section mainly originate from the integrated luminosity, photon and $\Lambda(\bar{\Lambda})$ reconstruction, $\Sigma^0(\bar{\Sigma}^0)$ mass window, background, angular distribution, branching fractions, and input line shape. The luminosity at each c.m. energy point is measured using Bhabha events, with the systematic uncertainty of 1.0% [61] below 4.0 GeV, 0.7% [62] from 4.0 to 4.6 GeV, and 0.5% [63] above 4.6 GeV. The systematic uncertainty due to the photon reconstruction is estimated to be 0.5% for each photon by analyzing the ISR process $e^+e^- \to \gamma\mu^+\mu^-$; the total systematic uncertainty due to photon reconstruction is considered as 1.0% summing up linearly the contribution from the two photons. The uncertainty due to the $\Lambda(\bar{\Lambda})$ reconstruction is obtained including the tracking and PID, the mass window, and the decay length uncertainties. This is studied using a control sample of $J/\psi \to pK^-\bar{\Lambda} +$ c.c. with the same method as used in Refs. [64–71] as a result, the efficiency difference between data and MC simulation is found to be 1.6% for the Λ reconstruction and 1.3% for the $\bar{\Lambda}$ reconstruction. The total uncertainty is 2.9% by adding them linearly. The uncertainty due to the Σ^0 mass window is estimated by varying the nominal requirements by 5 MeV/c^2, corresponding to an uncertainty of 1.0%. The uncertainty associated with the background estimation is assessed by shifting the sideband region outward or inward by 5 MeV/c^2, by summing up the samples from all the energy points to reduce the statistical fluctuations. The maximum deviation, 0.2%, is taken as the systematic uncertainty for background. The uncertainty due to the physical model dependence is estimated to be 2.2% by comparing the efficiency values obtained with the phase space model and using the real angular distribution, by incorporating the Σ^0 transverse polarization and the spin correlation based on the control sample $\psi(3686) \to \Sigma^0\bar{\Sigma}^0$. The uncertainty for the branching fractions of $\Lambda \to p\pi^-$ and $\bar{\Lambda} \to \bar{p}\pi^+$ is 1.6%, taken from the PDG [50]. The uncertainty due to the input line shape of the cross section when determining the ISR correction and the detection efficiency consists of two parts. One part is due to the statistical uncertainty of the input line shape of the cross section, estimated through an alternative input cross section line shape based on a simple power-law (PL) function by varying the central value of the fitted parameters by $\pm 1\sigma$. Another part of uncertainty for the input line shape arises from the resonance parameters of the assumed charmonium (-like) states, which are fixed according to the PDG values [50] in the fit of the cross section, and evaluated by varying the fixed values of the resonance parameters by 1σ uncertainty. Then, the $(1 + \delta)\epsilon$ value for each c.m. energy point is recalculated, and the largest change by considering

the contribution from the two parts is taken as the systematic uncertainty. The total systematic uncertainty due to the input line shape is calculated to be 2.0% by combining the contributions in quadrature.

The potential resonances in the cross section for the $e^+e^- \to \Sigma^0\bar{\Sigma}^0$ reaction are studied by fitting the dressed cross section, $\sigma^{\mathrm{dressed}} = \sigma^B/|1 - \Pi|^2$ (including the VP effect), using the least-squares method, where $\chi^2 = \Delta X^T V^{-1} \Delta X$. This is done by considering the covariance matrix V and the vector of residuals ΔX between the measured and fitted cross section. The covariance matrix incorporates both the correlated and uncorrelated uncertainties across different c.m. energies. The systematic uncertainties from luminosity, photon reconstruction, $\Lambda(\bar{\Lambda})$ reconstruction, Σ^0 mass window, background, and branching fraction are assumed to be fully correlated among different c.m. energies, while the other systematic uncertainties are assumed to be uncorrelated.

Assuming that the cross section of $e^+e^- \to \Sigma^0\bar{\Sigma}^0$ includes a resonance [i.e., $\psi(3770)$, $\psi(4040)$, $\psi(4160)$, $\psi(4230)$, $\psi(4360)$, $\psi(4415)$, or $\psi(4660)$] plus a contribution from the continuum processes, a fit to the dressed cross section is applied using the coherent sum of a power-law function plus a Breit-Wigner (BW) function [26]:

$$\sigma^{\mathrm{dressed}}(\sqrt{s}) = \left| c_0 \frac{\sqrt{P(\sqrt{s})}}{\sqrt{s^n}} + e^{i\phi}\mathrm{BW}(\sqrt{s})\sqrt{\frac{P(\sqrt{s})}{P(m)}} \right|^2. \quad (3)$$

Here, ϕ is the relative phase between the BW function

$$\mathrm{BW}(\sqrt{s}) = \frac{\sqrt{12\pi\Gamma_{ee}\mathcal{B}\Gamma}}{s - m^2 + im\Gamma} \quad (4)$$

and the PL function, c_0 and n are free parameters, $\sqrt{P(\sqrt{s})}$ is the two-body PHSP factor, the mass m, and the total width Γ are fixed to the PDG values [50] of the assumed resonance, and $\Gamma_{ee}\mathcal{B}$ is the product of the electronic partial width and the branching fraction for the resonance decaying into the $\Sigma^0\bar{\Sigma}^0$ final state. Figure 3 shows the fits to the dressed cross section under different resonance assumptions. The fit parameters with the assumption of no resonance are $c_0 = 1.8 \pm 0.9$ and $n = 8.5 \pm 0.4$. The resulting parameters under the different resonance assumptions are summarized in Table II, where the parameters of the PL contributions are omitted for readability. Considering the systematic uncertainties, the significance for each resonance is calculated by comparing the change of $\chi^2/$n.d.f (where n.d.f is the number of degrees of freedom) with and without the resonance assumption. The dressed cross section is fitted under different assumptions of charmonium(-like) states, i.e., $\psi(3770)$, $\psi(4040)$, $\psi(4160)$, $\psi(4230)$, $\psi(4360)$, $\psi(4415)$, and $\psi(4660)$, one at a time, by using Eq. (3). No obvious signal is found. The $\Gamma_{ee}\mathcal{B}$ and its upper limit including the
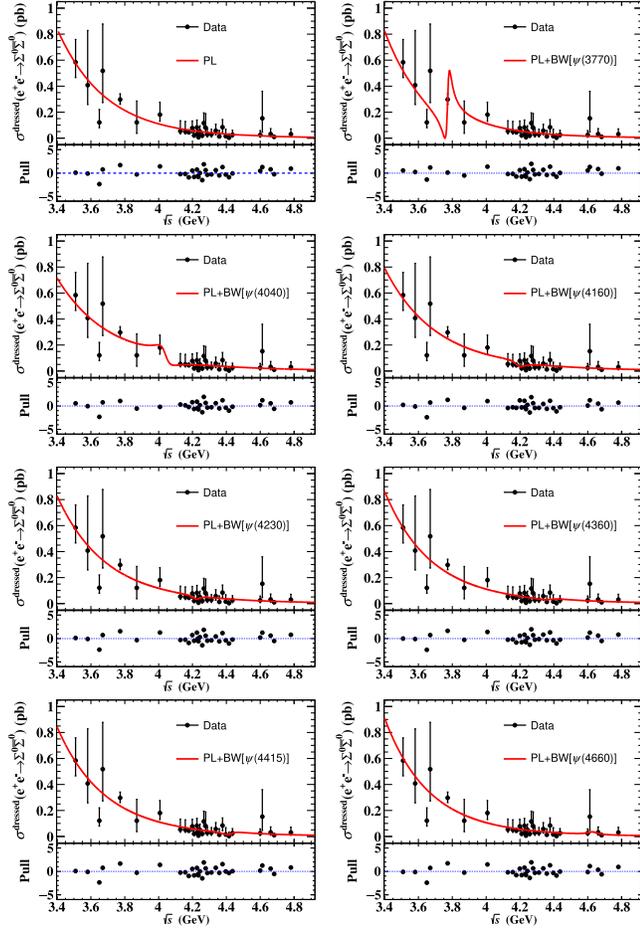
FIG. 3. Fits to the dressed cross section at c.m. energies from 3.510 to 4.951 GeV under different assumptions, as indicated in the legend. The dots with error bars represent the dressed cross section and the solid lines indicate the fit results. The error bars consider the statistical and systematic uncertainties summed in quadrature.

TABLE II. The fitted resonance parameters for $\Gamma_{ee}\mathcal{B}$ (10^{-3} eV) and ϕ (rad) for two solutions. The fit procedure includes both statistical and systematic uncertainties. Here the $\chi^2/\text{n.d.f.}$ indicates the fit quality for each assumed resonance.

Parameter	Solution I	Solution II	$\chi^2/\text{n.d.f.}$
$\phi_{\psi(3770)}$	-0.8 ± 0.1	-0.7 ± 0.1	$22/(32-4)$
$\Gamma_{ee}\mathcal{B}_{\psi(3770)}$	$17.2 \pm 1.4 (< 29.2)$	14.3 ± 1.1	
$\phi_{\psi(4040)}$	-1.9 ± 0.1	-3.0 ± 0.6	$23/(32-4)$
$\Gamma_{ee}\mathcal{B}_{\psi(4040)}$	$37.7 \pm 13.9 (< 66.1)$	3.6 ± 2.3	
$\phi_{\psi(4160)}$	-1.7 ± 0.1	-2.1 ± 0.3	$25/(32-4)$
$\Gamma_{ee}\mathcal{B}_{\psi(4160)}$	$17.7 \pm 2.4 (< 22.7)$	0.7 ± 0.7	
$\phi_{\psi(4230)}$	-1.6 ± 0.1	-1.6 ± 0.5	$26/(32-4)$
$\Gamma_{ee}\mathcal{B}_{\psi(4230)}$	$10.7 \pm 1.8 (< 14.7)$	0.2 ± 0.3	
$\phi_{\psi(4360)}$	-1.6 ± 1.8	-0.5 ± 1.1	$27/(32-4)$
$\Gamma_{ee}\mathcal{B}_{\psi(4360)}$	$20.9 \pm 11.5 (< 29.3)$	0.2 ± 0.5	
$\phi_{\psi(4415)}$	-1.5 ± 0.2	-0.9 ± 0.5	$27/(32-4)$
$\Gamma_{ee}\mathcal{B}_{\psi(4415)}$	$7.6 \pm 2.7 (< 14.0)$	0.5 ± 1.0	
$\phi_{\psi(4660)}$	-1.7 ± 0.3	1.7 ± 1.1	$27/(32-4)$
$\Gamma_{ee}\mathcal{B}_{\psi(4660)}$	$9.9 \pm 3.5 (< 17.4)$	0.5 ± 1.0	

$\psi(4415)$, or $\psi(4660)$] plus a continuum contribution. No significant signal is found. The products of branching fractions and electronic partial widths for these charmonium(-like) states decaying into the $\Sigma^0\bar{\Sigma}^0$ final state, as well as their upper limits at the 90% CL, are provided for the first time. In addition, the ratios of Born cross section and effective form factor of the $e^+e^- \to \Sigma^0\bar{\Sigma}^0$ reaction over the charged $e^+e^- \to \Sigma^+\bar{\Sigma}^-$ reaction are also provided, and the obtained results agree with the naive extrapolation of the theoretical prediction [36] to higher energies, and thereby can be used to validate the vector meson dominance model for these processes [39–43]. These results are important to study the vector charmonium(-like) states decaying into $B\bar{B}$ final states, and further investigate the nature of charmonium (-like) state production above the open-charm threshold.

systematic uncertainty at the 90% CL, computed using a Bayesian approach [72], are provided. The possible multiple solutions for the resonance parameters in the fit of the dressed cross section are obtained by scanning $\Gamma_{ee}\mathcal{B}$ and ϕ in the parameter space, and are provided in the Supplemental Material [52].

In summary, using e^+e^- collision data collected by the BESIII detector at the BEPCII collider corresponding to an integrated luminosity of 25 fb^{-1}, the Born cross section and the effective form factor for the $e^+e^- \to \Sigma^0\bar{\Sigma}^0$ reaction are measured at 32 c.m. energies ranging from 3.50 to 4.95 GeV for the first time. Our work provides not only better precision than the CLEO-c measurement at $\sqrt{s} = 3.770$ and 4.160 GeV [35], but also offers measurements at many points over a wide energy range. A fit to the dressed cross section of the $e^+e^- \to \Sigma^0\bar{\Sigma}^0$ reaction is performed under the assumption of a charmonium(-like) resonance [i.e., $\psi(3770)$, $\psi(4040)$, $\psi(4160)$, $\psi(4230)$, $\psi(4360)$,

Data availability. The data that support the findings of this article are not publicly available upon publication because it is not technically feasible and/or the cost of preparing, depositing, and hosting the data would be prohibitive within the terms of this research project. The data are available from the authors upon reasonable request.

[1] T. Barnes, S. Godfrey, and E. S. Swanson, Phys. Rev. D **72,** 054026 (2005).

[2] N. Brambilla *et al.*, Eur. Phys. J. C **71,** 1534 (2011).

[3] J. Z. Bai *et al.* (BES Collaboration), Phys. Rev. Lett. **88,** 101802 (2002).

[4] B. Aubert *et al.* (*BABAR* Collaboration), Phys. Rev. Lett. **95,** 142001 (2005).

[5] B. Aubert *et al.* (*BABAR* Collaboration), Phys. Rev. Lett. **98,** 212001 (2007).

[6] G. Pakhlova *et al.* (Belle Collaboration), Phys. Rev. Lett. **99,** 142002 (2007).

[7] G. Pakhlova *et al.* (Belle Collaboration), Phys. Rev. Lett. **99,** 182004 (2007).

[8] G. Pakhlova *et al.* (Belle Collaboration), Phys. Rev. Lett. **101,** 172001 (2008).

[9] B. Aubert *et al.* (*BABAR* Collaboration), Phys. Rev. D **86,** 051102 (2012).

[10] G. Pakhlova *et al.* (Belle Collaboration), Phys. Rev. Lett. **111,** 019901 (2013).

[11] B. Aubert *et al.* (*BABAR* Collaboration), Phys. Rev. D **89,** 111103 (2014).

[12] G. Pakhlova *et al.* (Belle Collaboration), Phys. Rev. D **91,** 112007 (2015).

[13] T. E. Coan *et al.* (CLEO Collaboration), Phys. Rev. Lett. **96,** 162003 (2006).

[14] M. Ablikim *et al.* (BESIII Collaboration), Phys. Rev. Lett. **114,** 092003 (2015).

[15] M. Ablikim *et al.* (BESIII Collaboration), Phys. Rev. Lett. **130,** 121901 (2023).

[16] M. Ablikim *et al.* (BESIII Collaboration), Phys. Rev. Lett. **133,** 081901 (2024).

[17] H. X. Chen, W. Chen, X. Liu, and S. L. Zhu, Phys. Rep. **639,** 1 (2016).

[18] R. A. Briceno *et al.*, Chin. Phys. C **40,** 042001 (2016).

[19] F. E. Close and P. R. Page, Phys. Lett. B **628,** 215 (2005).

[20] M. Cleven, Q. Wang, F. K. Guo, C. Hanhart, U. G. Meißner, and Q. Zhao, Phys. Rev. D **90,** 074039 (2014).

[21] J. Z. Wang, D. Y. Chen, X. Liu, and T. Matsuki, Phys. Rev. D **99,** 114003 (2019).

[22] R. Q. Qian, Q. Huang, and X. Liu, Phys. Lett. B **833,** 137292 (2022).

[23] R. Baldini Ferroli, A. Mangoni, S. Pacetti, and K. Zhu, Phys. Lett. B **799,** 135041 (2019).

[24] M. Ablikim *et al.* (BESIII Collaboration), Phys. Rev. D **87,** 112011 (2013).

[25] M. Ablikim *et al.* (BESIII Collaboration), Phys. Rev. Lett. **120,** 132001 (2018).

[26] M. Ablikim *et al.* (BESIII Collaboration), Phys. Rev. Lett. **124,** 032002 (2020).

[27] M. Ablikim *et al.* (BESIII Collaboration), Phys. Rev. D **104,** L091104 (2021).

[28] M. Ablikim *et al.* (BESIII Collaboration), Phys. Lett. B **820,** 136557 (2021).

[29] M. Ablikim *et al.* (BESIII Collaboration), Phys. Rev. D **105,** L011101 (2022).

[30] M. Ablikim *et al.* (BESIII Collaboration), J. High Energy Phys. 11 (2023) 228.

[31] M. Ablikim *et al.* (BESIII Collaboration), Phys. Rev. Lett. **131,** 191901 (2023).

[32] M. Ablikim *et al.* (BESIII Collaboration), J. High Energy Phys. 05 (2024) 022.

[33] M. Ablikim *et al.* (BESIII Collaboration), J. High Energy Phys. 07 (2024) 258.

[34] M. Ablikim *et al.* (BESIII Collaboration), J. High Energy Phys. 11 (2024) 062.

[35] S. Dobbs, K. K. Seth, A. Tomaradze, T. Xiao, and G. Bonvicini, Phys. Rev. D **96,** 092004 (2017).

[36] B. Yan, C. Chen, and J. J. Xie, Phys. Rev. D **107,** 076008 (2023).

[37] J. P. Dai, X. Cao, and H. Lenske, Phys. Lett. B **846,** 138192 (2023).

[38] Y. Z. Xu, S. Y. Chen, Z. Q. Yao, D. Binosi, Z.-F. Cui, and C. D. Roberts, Eur. Phys. J. C **81**, 895 (2021).

[39] F. Iachello, A. D. Jackson, and A. Lande, Phys. Lett. **43B**, 191 (1973).

[40] F. Iachello and Q. Wan, Phys. Rev. C **69**, 055204 (2004).

[41] R. Bijker and F. Iachello, Phys. Rev. C **69**, 068201 (2004).

[42] Y. Yang, D. Y. Chen, and Z. Lu, Phys. Rev. D **100**, 073007 (2019).

[43] Z. Y. Li, A. X. Dai, and J. J. Xie, Chin. Phys. Lett. **39**, L011201 (2022).

[44] M. Ablikim *et al.* (BESIII Collaboration), Nucl. Instrum. Methods Phys. Res., Sect. A **614**, 345 (2010).

[45] C. Yu *et al.*, in *Proceedings of International Particle Accelerator Conference (IPAC'16)*, (2016).

[46] S. Jadach, B. F. L. Ward, and Z. Was, Phys. Rev. D **63**, 113009 (2001).

[47] D. J. Lange, Nucl. Instrum. Methods Phys. Res., Sect. A **462**, 152 (2001).

[48] R. G. Ping, Chin. Phys. C **32**, 599 (2008).

[49] S. Agostinelli *et al.* (GEANT4 Collaboration), Nucl. Instrum. Methods Phys. Res., Sect. A **506**, 250 (2003).

[50] R. L. Workman *et al.* (Particle Data Group), Prog. Theor. Exp. Phys. **2022**, 083C01 (2022).

[51] J. Lundberg, J. Conrad, W. Rolke, and A. Lopez, Comput. Phys. Commun. **181**, 683 (2010).

[52] See Supplemental Material at http://link.aps.org/supplemental/10.1103/PhysRevD.111.L051502 for a summary of luminosity, ISR factor, vacuum polarization factor, detection efficiency, number of signal events, the Born cross section, the effective form factor, significance at each energy point, which includes Refs. [53,54].

[53] M. Ablikim *et al.* (BESIII Collaboration), Chin. Phys. C **40**, 063001 (2016).

[54] M. Ablikim *et al.* (BESIII Collaboration), Chin. Phys. C **45**, 103001 (2021).

[55] E. A. Kuraev and V. S. Fadin, Sov. J. Nucl. Phys. **41**, 466 (1985).

[56] F. Jegerlehner and R. Szafron, Eur. Phys. J. C **71**, 1632 (2011).

[57] W. Sun, T. Liu, M. Jing, L. Wang, B. Zhong, and W. Song, Front. Phys. (Beijing) **16**, 64501 (2021).

[58] X. F. Wang and G. S. Huang, Symmetry **14**, 65 (2022).

[59] R. Baldini, S. Pacetti, A. Zallo, and A. Zichichi, Eur. Phys. J. A **39**, 315 (2009).

[60] A. B. Arbuzov and T. V. Kopylova, J. High Energy Phys. 04 (2012) 009.

[61] M. Ablikim *et al.* (BESIII Collaboration), Chin. Phys. C **39**, 093001 (2015).

[62] M. Ablikim *et al.* (BESIII Collaboration), Chin. Phys. C **46**, 113002 (2022).

[63] M. Ablikim *et al.* (BESIII Collaboration), Chin. Phys. C **46**, 113003 (2022).

[64] M. Ablikim *et al.* (BESIII Collaboration), Phys. Rev. D **93**, 072003 (2016).

[65] M. Ablikim *et al.* (BESIII Collaboration), Phys. Lett. B **770**, 217 (2017).

[66] M. Ablikim *et al.* (BESIII Collaboration), Phys. Rev. D **100**, 051101 (2019).

[67] M. Ablikim *et al.* (BESIII Collaboration), J. High Energy Phys. 06 (2022) 74.

[68] M. Ablikim *et al.* (BESIII Collaboration), Phys. Rev. D **106**, L091101 (2022).

[69] M. Ablikim *et al.* (BESIII Collaboration), Phys. Rev. D **108**, L011101 (2023).

[70] M. Ablikim *et al.* (BESIII Collaboration), J. High Energy Phys. 10 (2023) 081; 12 (2023) 080(E).

[71] M. Ablikim *et al.* (BESIII Collaboration), Phys. Rev. D **108**, L031106 (2023).

[72] Y. S. Zhu, Chin. Phys. C **32**, 363 (2008).

M. Ablikim,[1] M. N. Achasov,[4,c] P. Adlarson,[76] O. Afedulidis,[3] X. C. Ai,[81] R. Aliberti,[35] A. Amoroso,[75a,75c] Y. Bai,[57] O. Bakina,[36] I. Balossino,[29a] Y. Ban,[46,h] H.-R. Bao,[64] V. Batozskaya,[1,44] K. Begzsuren,[32] N. Berger,[35] M. Berlowski,[44] M. Bertani,[28a] D. Bettoni,[29a] F. Bianchi,[75a,75c] E. Bianco,[75a,75c] A. Bortone,[75a,75c] I. Boyko,[36] R. A. Briere,[5] A. Brueggemann,[69] H. Cai,[77] M. H. Cai,[38,k,l] X. Cai,[1,58] A. Calcaterra,[28a] G. F. Cao,[1,64] N. Cao,[1,64] S. A. Cetin,[62a] X. Y. Chai,[46,h] J. F. Chang,[1,58] G. R. Che,[43] Y. Z. Che,[1,58,64] G. Chelkov,[36,b] C. Chen,[43] C. H. Chen,[9] Chao Chen,[55] G. Chen,[1] H. S. Chen,[1,64] H. Y. Chen,[20] M. L. Chen,[1,58,64] S. J. Chen,[42] S. L. Chen,[45] S. M. Chen,[61] T. Chen,[1,64] X. R. Chen,[31,64] X. T. Chen,[1,64] Y. B. Chen,[1,58] Y. Q. Chen,[34] Z. J. Chen,[25,i] Z. Y. Chen,[1,64] S. K. Choi,[10] G. Cibinetto,[29a] F. Cossio,[75c] J. J. Cui,[50] H. L. Dai,[1,58] J. P. Dai,[79] A. Dbeyssi,[18] R. E. de Boer,[3] D. Dedovich,[36] C. Q. Deng,[73] Z. Y. Deng,[1] A. Denig,[35] I. Denysenko,[36] M. Destefanis,[75a,75c] F. De Mori,[75a,75c] B. Ding,[67,1] X. X. Ding,[46,h] Y. Ding,[40] Y. Ding,[34] J. Dong,[1,58] L. Y. Dong,[1,64] M. Y. Dong,[1,58,64] X. Dong,[77] M. C. Du,[1] S. X. Du,[81] Y. Y. Duan,[55] Z. H. Duan,[42] P. Egorov,[36,b] Y. H. Fan,[45] J. Fang,[1,58] J. Fang,[59] S. S. Fang,[1,64] W. X. Fang,[1] Y. Fang,[1] Y. Q. Fang,[1,58] R. Farinelli,[29a] L. Fava,[75b,75c] F. Feldbauer,[3] G. Felici,[28a] C. Q. Feng,[72,58] J. H. Feng,[59] Y. T. Feng,[72,58] M. Fritsch,[3] C. D. Fu,[1] J. L. Fu,[64] Y. W. Fu,[1,64] H. Gao,[64] X. B. Gao,[41] Y. N. Gao,[46,h] Yang Gao,[72,58] S. Garbolino,[75c] I. Garzia,[29a,29b] L. Ge,[81] P. T. Ge,[19] Z. W. Ge,[42] C. Geng,[59] E. M. Gersabeck,[68] A. Gilman,[70] K. Goetzen,[13] L. Gong,[40] W. X. Gong,[1,58] W. Gradl,[35] S. Gramigna,[29a,29b] M. Greco,[75a,75c] M. H. Gu,[1,58] Y. T. Gu,[15] C. Y. Guan,[1,64] A. Q. Guo,[31,64] L. B. Guo,[41] M. J. Guo,[50] R. P. Guo,[49] Y. P. Guo,[12,g] A. Guskov,[36,b] J. Gutierrez,[27] K. L. Han,[64] T. T. Han,[1] F. Hanisch,[3] X. Q. Hao,[19] F. A. Harris,[66] K. K. He,[55] K. L. He,[1,64] F. H. Heinsius,[3] C. H. Heinz,[35] Y. K. Heng,[1,58,64] C. Herold,[60] T. Holtmann,[3] P. C. Hong,[34] G. Y. Hou,[1,64] X. T. Hou,[1,64] Y. R. Hou,[64]

Z. L. Hou,[1] B. Y. Hu,[59] H. M. Hu,[1,64] J. F. Hu,[56,j] Q. P. Hu,[72,58] S. L. Hu,[12,g] T. Hu,[1,58,64] Y. Hu,[1] G. S. Huang,[72,58] K. X. Huang,[59] L. Q. Huang,[31,64] X. T. Huang,[50] Y. P. Huang,[1] Y. S. Huang,[59] T. Hussain,[74] F. Hölzken,[3] N. Hüsken,[35] N. in der Wiesche,[69] J. Jackson,[27] S. Janchiv,[32] J. H. Jeong,[10] Q. Ji,[1] Q. P. Ji,[19] W. Ji,[1,64] X. B. Ji,[1,64] X. L. Ji,[1,58] Y. Y. Ji,[50] X. Q. Jia,[50] Z. K. Jia,[72,58] D. Jiang,[1,64] H. B. Jiang,[77] P. C. Jiang,[46,h] S. S. Jiang,[39] T. J. Jiang,[16] X. S. Jiang,[1,58,64] Y. Jiang,[64] J. B. Jiao,[50] J. K. Jiao,[34] Z. Jiao,[23] S. Jin,[42] Y. Jin,[67] M. Q. Jing,[1,64] X. M. Jing,[64] T. Johansson,[76] S. Kabana,[33] N. Kalantar-Nayestanaki,[65] X. L. Kang,[9] X. S. Kang,[40] M. Kavatsyuk,[65] B. C. Ke,[81] V. Khachatryan,[27] A. Khoukaz,[69] R. Kiuchi,[1] O. B. Kolcu,[62a] B. Kopf,[3] M. Kuessner,[3] X. Kui,[1,64] N. Kumar,[26] A. Kupsc,[44,76] W. Kühn,[37] L. Lavezzi,[75a,75c] T. T. Lei,[72,58] Z. H. Lei,[72,58] M. Lellmann,[35] T. Lenz,[35] C. Li,[43] C. Li,[47] C. H. Li,[39] Cheng Li,[72,58] D. M. Li,[81] F. Li,[1,58] G. Li,[1] H. B. Li,[1,64] H. J. Li,[19] H. N. Li,[56,j] Hui Li,[43] J. R. Li,[61] J. S. Li,[59] K. Li,[1] K. L. Li,[19] L. J. Li,[1,64] L. K. Li,[1] Lei Li,[48] M. H. Li,[43] P. R. Li,[38,k,l] Q. M. Li,[1,64] Q. X. Li,[50] R. Li,[17,31] S. X. Li,[12] T. Li,[50] T. Y. Li,[43] W. D. Li,[1,64] W. G. Li,[1,a] X. Li,[1,64] X. H. Li,[72,58] X. L. Li,[50] X. Y. Li,[1,8] X. Z. Li,[59] Y. G. Li,[46,h] Z. J. Li,[59] Z. Y. Li,[79] C. Liang,[42] H. Liang,[72,58] H. Liang,[1,64] Y. F. Liang,[54] Y. T. Liang,[31,64] G. R. Liao,[14] Y. P. Liao,[1,64] J. Libby,[26] A. Limphirat,[60] C. C. Lin,[55] C. X. Lin,[64] D. X. Lin,[31,64] T. Lin,[1] B. J. Liu,[1] B. X. Liu,[77] C. Liu,[34] C. X. Liu,[1] F. Liu,[1] F. H. Liu,[53] Feng Liu,[6] G. M. Liu,[56,j] H. Liu,[38,k,l] H. B. Liu,[15] H. H. Liu,[1] H. M. Liu,[1,64] Huihui Liu,[21] J. B. Liu,[72,58] J. Y. Liu,[1,64] K. Liu,[38,k,l] K. Y. Liu,[40] Ke Liu,[22] L. Liu,[72,58] L. C. Liu,[43] Lu Liu,[43] M. H. Liu,[12,g] P. L. Liu,[1] Q. Liu,[64] S. B. Liu,[72,58] T. Liu,[12,g] W. K. Liu,[43] W. M. Liu,[72,58] X. Liu,[38,k,l] X. Liu,[39] Y. Liu,[81] Y. Liu,[38,k,l] Y. B. Liu,[43] Z. A. Liu,[1,58,64] Z. D. Liu,[9] Z. Q. Liu,[50] X. C. Lou,[1,58,64] F. X. Lu,[59] H. J. Lu,[23] J. G. Lu,[1,58] X. L. Lu,[1] Y. Lu,[7] Y. P. Lu,[1,58] Z. H. Lu,[1,64] C. L. Luo,[41] J. R. Luo,[59] M. X. Luo,[80] T. Luo,[12,g] X. L. Luo,[1,58] X. R. Lyu,[64] Y. F. Lyu,[43] F. C. Ma,[40] H. Ma,[79] H. L. Ma,[1] J. L. Ma,[1,64] L. L. Ma,[50] L. R. Ma,[67] M. M. Ma,[1,64] Q. M. Ma,[1] R. Q. Ma,[1,64] T. Ma,[72,58] X. T. Ma,[1,64] X. Y. Ma,[1,58] Y. M. Ma,[31] F. E. Maas,[18] I. MacKay,[70] M. Maggiora,[75a,75c] S. Malde,[70] Y. J. Mao,[46,h] Z. P. Mao,[1] S. Marcello,[75a,75c] Z. X. Meng,[67] J. G. Messchendorp,[13,65] G. Mezzadri,[29a] H. Miao,[1,64] T. J. Min,[42] R. E. Mitchell,[27] X. H. Mo,[1,58,64] B. Moses,[27] N. Yu. Muchnoi,[4,c] J. Muskalla,[35] Y. Nefedov,[36] F. Nerling,[18,e] L. S. Nie,[20] I. B. Nikolaev,[4,c] Z. Ning,[1,58] S. Nisar,[11,m] Q. L. Niu,[38,k,l] W. D. Niu,[55] Y. Niu,[50] S. L. Olsen,[64] S. L. Olsen,[10,64] Q. Ouyang,[1,58,64] S. Pacetti,[28b,28c] X. Pan,[55] Y. Pan,[57] A. Pathak,[34] Y. P. Pei,[72,58] M. Pelizaeus,[3] H. P. Peng,[72,58] Y. Y. Peng,[38,k,l] K. Peters,[13,e] J. L. Ping,[41] R. G. Ping,[1,64] S. Plura,[35] V. Prasad,[33] F. Z. Qi,[1] H. Qi,[72,58] H. R. Qi,[61] M. Qi,[42] T. Y. Qi,[12,g] S. Qian,[1,58] W. B. Qian,[64] C. F. Qiao,[64] X. K. Qiao,[81] J. J. Qin,[73] L. Q. Qin,[14] L. Y. Qin,[72,58] X. P. Qin,[12,g] X. S. Qin,[50] Z. H. Qin,[1,58] J. F. Qiu,[1] Z. H. Qu,[73] C. F. Redmer,[35] K. J. Ren,[39] A. Rivetti,[75c] M. Rolo,[75c] G. Rong,[1,64] Ch. Rosner,[18] M. Q. Ruan,[1,58] S. N. Ruan,[43] N. Salone,[44] A. Sarantsev,[36,d] Y. Schelhaas,[35] K. Schoenning,[76] M. Scodeggio,[29a] K. Y. Shan,[12,g] W. Shan,[24] X. Y. Shan,[72,58] Z. J. Shang,[38,k,l] J. F. Shangguan,[16] L. G. Shao,[1,64] M. Shao,[72,58] C. P. Shen,[12,g] H. F. Shen,[1,8] W. H. Shen,[64] X. Y. Shen,[1,64] B. A. Shi,[64] H. Shi,[72,58] J. L. Shi,[12,g] J. Y. Shi,[1] Q. Q. Shi,[55] S. Y. Shi,[73] X. Shi,[1,58] J. J. Song,[19] T. Z. Song,[59] W. M. Song,[34,1] Y. J. Song,[12,g] Y. X. Song,[46,h,n] S. Sosio,[75a,75c] S. Spataro,[75a,75c] F. Stieler,[35] S. S. Su,[40] Y. J. Su,[64] G. B. Sun,[77] G. X. Sun,[1] H. Sun,[64] H. K. Sun,[1] J. F. Sun,[19] K. Sun,[61] L. Sun,[77] S. S. Sun,[1,64] T. Sun,[51,f] W. Y. Sun,[34] Y. Sun,[9] Y. J. Sun,[72,58] Y. Z. Sun,[1] Z. Q. Sun,[1,64] Z. T. Sun,[50] C. J. Tang,[54] G. Y. Tang,[1] J. Tang,[59] M. Tang,[72,58] Y. A. Tang,[77] L. Y. Tao,[73] Q. T. Tao,[25,i] M. Tat,[70] J. X. Teng,[72,58] V. Thoren,[76] W. H. Tian,[59] Y. Tian,[31,64] Z. F. Tian,[77] I. Uman,[62b] Y. Wan,[55] S. J. Wang,[50] B. Wang,[1] B. L. Wang,[64] Bo Wang,[72,58] D. Y. Wang,[46,h] F. Wang,[73] H. J. Wang,[38,k,l] J. J. Wang,[77] J. P. Wang,[50] K. Wang,[1,58] L. L. Wang,[1] M. Wang,[50] N. Y. Wang,[64] S. Wang,[12,g] S. Wang,[38,k,l] T. Wang,[12,g] T. J. Wang,[43] W. Wang,[59] W. Wang,[73] W. P. Wang,[35,58,72,o] X. Wang,[46,h] X. F. Wang,[38,k,l] X. J. Wang,[39] X. L. Wang,[12,g] X. N. Wang,[1] Y. Wang,[61] Y. D. Wang,[45] Y. F. Wang,[1,58,64] Y. H. Wang,[38,k,l] Y. L. Wang,[19] Y. N. Wang,[45] Y. Q. Wang,[1] Yaqian Wang,[17] Yi Wang,[61] Z. Wang,[1,58] Z. L. Wang,[73] Z. Y. Wang,[1,64] Ziyi Wang,[64] D. H. Wei,[14] F. Weidner,[69] S. P. Wen,[1] Y. R. Wen,[39] U. Wiedner,[3] G. Wilkinson,[70] M. Wolke,[76] L. Wollenberg,[3] C. Wu,[39] J. F. Wu,[1,8] L. H. Wu,[1] L. J. Wu,[1,64] X. Wu,[12,g] X. H. Wu,[34] Y. Wu,[72,58] Y. H. Wu,[55] Y. J. Wu,[31] Z. Wu,[1,58] L. Xia,[72,58] X. M. Xian,[39] B. H. Xiang,[1,64] T. Xiang,[46,h] D. Xiao,[38,k,l] G. Y. Xiao,[42] S. Y. Xiao,[1] Y. L. Xiao,[12,g] Z. J. Xiao,[41] C. Xie,[42] X. H. Xie,[46,h] Y. Xie,[50] Y. G. Xie,[1,58] Y. H. Xie,[6] Z. P. Xie,[72,58] T. Y. Xing,[1,64] C. F. Xu,[1,64] C. J. Xu,[59] G. F. Xu,[1] H. Y. Xu,[67,2] M. Xu,[72,58] Q. J. Xu,[16] Q. N. Xu,[30] W. Xu,[1] W. L. Xu,[67] X. P. Xu,[55] Y. Xu,[40] Y. C. Xu,[78] Z. S. Xu,[64] F. Yan,[12,g] L. Yan,[12,g] W. B. Yan,[72,58] W. C. Yan,[81] X. Q. Yan,[1,64] H. J. Yang,[51,f] H. L. Yang,[34] H. X. Yang,[1] J. H. Yang,[42] T. Yang,[1] Y. Yang,[12,g] Y. F. Yang,[1,64] Y. F. Yang,[43] Y. X. Yang,[1,64] Z. W. Yang,[38,k,l] Z. P. Yao,[50] M. Ye,[1,58] M. H. Ye,[8] J. H. Yin,[1] Junhao Yin,[43] Z. Y. You,[59] B. X. Yu,[1,58,64] C. X. Yu,[43] G. Yu,[1,64] J. S. Yu,[25,i] M. C. Yu,[40] T. Yu,[73] X. D. Yu,[46,h] Y. C. Yu,[81] C. Z. Yuan,[1,64] J. Yuan,[45] J. Yuan,[34] L. Yuan,[2] S. C. Yuan,[1,64] Y. Yuan,[1,64] Z. Y. Yuan,[59] C. X. Yue,[39] A. A. Zafar,[74] F. R. Zeng,[50] S. H. Zeng,[63] X. Zeng,[12,g] Y. Zeng,[25,i] Y. J. Zeng,[1,64] Y. J. Zeng,[59] X. Y. Zhai,[34] Y. C. Zhai,[50] Y. H. Zhan,[59] A. Q. Zhang,[1,64] B. L. Zhang,[1,64] B. X. Zhang,[1] D. H. Zhang,[43] G. Y. Zhang,[19] H. Zhang,[81] H. Zhang,[72,58] H. C. Zhang,[1,58,64] H. H. Zhang,[34] H. H. Zhang,[59] H. Q. Zhang,[1,58,64] H. R. Zhang,[72,58]

H. Y. Zhang,[1,58] J. Zhang,[81] J. Zhang,[59] J. J. Zhang,[52] J. L. Zhang,[20] J. Q. Zhang,[41] J. S. Zhang,[12,g] J. W. Zhang,[1,58,64] J. X. Zhang,[38,k,l] J. Y. Zhang,[1] J. Z. Zhang,[1,64] Jianyu Zhang,[64] L. M. Zhang,[61] Lei Zhang,[42] P. Zhang,[1,64] Q. Y. Zhang,[34] R. Y. Zhang,[38,k,l] S. H. Zhang,[1,64] Shulei Zhang,[25,i] X. M. Zhang,[1] X. Y. Zhang,[40] X. Y. Zhang,[50] Y. Zhang,[1] Y. Zhang,[73] Y. T. Zhang,[81] Y. H. Zhang,[1,58] Y. M. Zhang,[39] Yan Zhang,[72,58] Z. D. Zhang,[1] Z. H. Zhang,[1] Z. L. Zhang,[34] Z. Y. Zhang,[43] Z. Y. Zhang,[77] Z. Z. Zhang,[45] G. Zhao,[1] J. Y. Zhao,[1,64] J. Z. Zhao,[1,58] L. Zhao,[1] Lei Zhao,[72,58] M. G. Zhao,[43] N. Zhao,[79] R. P. Zhao,[64] S. J. Zhao,[81] Y. B. Zhao,[1,58] Y. X. Zhao,[31,64] Z. G. Zhao,[72,58] A. Zhemchugov,[36,b] B. Zheng,[73] B. M. Zheng,[34] J. P. Zheng,[1,58] W. J. Zheng,[1,64] Y. H. Zheng,[64] B. Zhong,[41] X. Zhong,[59] H. Zhou,[50] J. Y. Zhou,[34] L. P. Zhou,[1,64] S. Zhou,[6] X. Zhou,[77] X. K. Zhou,[6] X. R. Zhou,[72,58] X. Y. Zhou,[39] Y. Z. Zhou,[12,g] Z. C. Zhou,[20] A. N. Zhu,[64] J. Zhu,[43] K. Zhu,[1] K. J. Zhu,[1,58,64] K. S. Zhu,[12,g] L. Zhu,[34] L. X. Zhu,[64] S. H. Zhu,[71] T. J. Zhu,[12,g] W. D. Zhu,[41] Y. C. Zhu,[72,58] Z. A. Zhu,[1,64] J. H. Zou,[1] and J. Zu[72,58]

(BESIII Collaboration)

[1]Institute of High Energy Physics, Beijing 100049, People's Republic of China
[2]Beihang University, Beijing 100191, People's Republic of China
[3]Bochum Ruhr-University, D-44780 Bochum, Germany
[4]Budker Institute of Nuclear Physics SB RAS (BINP), Novosibirsk 630090, Russia
[5]Carnegie Mellon University, Pittsburgh, Pennsylvania 15213, USA
[6]Central China Normal University, Wuhan 430079, People's Republic of China
[7]Central South University, Changsha 410083, People's Republic of China
[8]China Center of Advanced Science and Technology, Beijing 100190, People's Republic of China
[9]China University of Geosciences, Wuhan 430074, People's Republic of China
[10]Chung-Ang University, Seoul, 06974, Republic of Korea
[11]COMSATS University Islamabad, Lahore Campus,
Defence Road, Off Raiwind Road, 54000 Lahore, Pakistan
[12]Fudan University, Shanghai 200433, People's Republic of China
[13]GSI Helmholtzcentre for Heavy Ion Research GmbH, D-64291 Darmstadt, Germany
[14]Guangxi Normal University, Guilin 541004, People's Republic of China
[15]Guangxi University, Nanning 530004, People's Republic of China
[16]Hangzhou Normal University, Hangzhou 310036, People's Republic of China
[17]Hebei University, Baoding 071002, People's Republic of China
[18]Helmholtz Institute Mainz, Staudinger Weg 18, D-55099 Mainz, Germany
[19]Henan Normal University, Xinxiang 453007, People's Republic of China
[20]Henan University, Kaifeng 475004, People's Republic of China
[21]Henan University of Science and Technology, Luoyang 471003, People's Republic of China
[22]Henan University of Technology, Zhengzhou 450001, People's Republic of China
[23]Huangshan College, Huangshan 245000, People's Republic of China
[24]Hunan Normal University, Changsha 410081, People's Republic of China
[25]Hunan University, Changsha 410082, People's Republic of China
[26]Indian Institute of Technology Madras, Chennai 600036, India
[27]Indiana University, Bloomington, Indiana 47405, USA
[28a]INFN Laboratori Nazionali di Frascati, I-00044, Frascati, Italy
[28b]INFN Sezione di Perugia, I-06100, Perugia, Italy
[28c]University of Perugia, I-06100, Perugia, Italy
[29a]INFN Sezione di Ferrara, I-44122, Ferrara, Italy
[29b]University of Ferrara, I-44122, Ferrara, Italy
[30]Inner Mongolia University, Hohhot 010021, People's Republic of China
[31]Institute of Modern Physics, Lanzhou 730000, People's Republic of China
[32]Institute of Physics and Technology, Peace Avenue 54B, Ulaanbaatar 13330, Mongolia
[33]Instituto de Alta Investigación, Universidad de Tarapacá, Casilla 7D, Arica 1000000, Chile
[34]Jilin University, Changchun 130012, People's Republic of China
[35]Johannes Gutenberg University of Mainz, Johann-Joachim-Becher-Weg 45, D-55099 Mainz, Germany
[36]Joint Institute for Nuclear Research, 141980 Dubna, Moscow region, Russia
[37]Justus-Liebig-Universitaet Giessen, II. Physikalisches Institut,
Heinrich-Buff-Ring 16, D-35392 Giessen, Germany
[38]Lanzhou University, Lanzhou 730000, People's Republic of China
[39]Liaoning Normal University, Dalian 116029, People's Republic of China

[40]*Liaoning University, Shenyang 110036, People's Republic of China*

[41]*Nanjing Normal University, Nanjing 210023, People's Republic of China*

[42]*Nanjing University, Nanjing 210093, People's Republic of China*

[43]*Nankai University, Tianjin 300071, People's Republic of China*

[44]*National Centre for Nuclear Research, Warsaw 02-093, Poland*

[45]*North China Electric Power University, Beijing 102206, People's Republic of China*

[46]*Peking University, Beijing 100871, People's Republic of China*

[47]*Qufu Normal University, Qufu 273165, People's Republic of China*

[48]*Renmin University of China, Beijing 100872, People's Republic of China*

[49]*Shandong Normal University, Jinan 250014, People's Republic of China*

[50]*Shandong University, Jinan 250100, People's Republic of China*

[51]*Shanghai Jiao Tong University, Shanghai 200240, People's Republic of China*

[52]*Shanxi Normal University, Linfen 041004, People's Republic of China*

[53]*Shanxi University, Taiyuan 030006, People's Republic of China*

[54]*Sichuan University, Chengdu 610064, People's Republic of China*

[55]*Soochow University, Suzhou 215006, People's Republic of China*

[56]*South China Normal University, Guangzhou 510006, People's Republic of China*

[57]*Southeast University, Nanjing 211100, People's Republic of China*

[58]*State Key Laboratory of Particle Detection and Electronics,*
Beijing 100049, Hefei 230026, People's Republic of China

[59]*Sun Yat-Sen University, Guangzhou 510275, People's Republic of China*

[60]*Suranaree University of Technology, University Avenue 111, Nakhon Ratchasima 30000, Thailand*

[61]*Tsinghua University, Beijing 100084, People's Republic of China*

[62a]*Turkish Accelerator Center Particle Factory Group, Istinye University, 34010, Istanbul, Turkey*

[62b]*Near East University, Nicosia, North Cyprus, 99138, Mersin 10, Turkey*

[63]*University of Bristol, H H Wills Physics Laboratory, Tyndall Avenue, Bristol BS8 1TL, United Kingdom*

[64]*University of Chinese Academy of Sciences, Beijing 100049, People's Republic of China*

[65]*University of Groningen, NL-9747 AA Groningen, The Netherlands*

[66]*University of Hawaii, Honolulu, Hawaii 96822, USA*

[67]*University of Jinan, Jinan 250022, People's Republic of China*

[68]*University of Manchester, Oxford Road, Manchester, M13 9PL, United Kingdom*

[69]*University of Muenster, Wilhelm-Klemm-Strasse 9, 48149 Muenster, Germany*

[70]*University of Oxford, Keble Road, Oxford OX13RH, United Kingdom*

[71]*University of Science and Technology Liaoning, Anshan 114051, People's Republic of China*

[72]*University of Science and Technology of China, Hefei 230026, People's Republic of China*

[73]*University of South China, Hengyang 421001, People's Republic of China*

[74]*University of the Punjab, Lahore-54590, Pakistan*

[75a]*University of Turin and INFN, University of Turin, I-10125, Turin, Italy*

[75b]*University of Eastern Piedmont, I-15121, Alessandria, Italy*

[75c]*INFN, I-10125, Turin, Italy*

[76]*Uppsala University, Box 516, SE-75120 Uppsala, Sweden*

[77]*Wuhan University, Wuhan 430072, People's Republic of China*

[78]*Yantai University, Yantai 264005, People's Republic of China*

[79]*Yunnan University, Kunming 650500, People's Republic of China*

[80]*Zhejiang University, Hangzhou 310027, People's Republic of China*

[81]*Zhengzhou University, Zhengzhou 450001, People's Republic of China*

[a]Deceased.

[b]Also at the Moscow Institute of Physics and Technology, Moscow 141700, Russia.

[c]Also at the Novosibirsk State University, Novosibirsk, 630090, Russia.

[d]Also at the NRC "Kurchatov Institute," PNPI, 188300, Gatchina, Russia.

[e]Also at Goethe University Frankfurt, 60323 Frankfurt am Main, Germany.

[f]Also at Key Laboratory for Particle Physics, Astrophysics and Cosmology, Ministry of Education; Shanghai Key Laboratory for Particle Physics and Cosmology; Institute of Nuclear and Particle Physics, Shanghai 200240, People's Republic of China.

[g]Also at Key Laboratory of Nuclear Physics and Ion-beam Application (MOE) and Institute of Modern Physics, Fudan University, Shanghai 200443, People's Republic of China.

[h]Also at State Key Laboratory of Nuclear Physics and Technology, Peking University, Beijing 100871, People's Republic of China.

[i]Also at School of Physics and Electronics, Hunan University, Changsha 410082, China.

[j]Also at Guangdong Provincial Key Laboratory of Nuclear Science, Institute of Quantum Matter, South China Normal University, Guangzhou 510006, China.

[k]Also at MOE Frontiers Science Center for Rare Isotopes, Lanzhou University, Lanzhou 730000, People's Republic of China.

[l]Also at Lanzhou Center for Theoretical Physics, Key Laboratory of Theoretical Physics of Gansu Province, and Key Laboratory for Quantum Theory and Applications of MoE, Gansu Provincial Research Center for Basic Disciplines of Quantum Physics, Lanzhou University, Lanzhou 730000, People's Republic of China.

[m]Also at the Department of Mathematical Sciences, IBA, Karachi 75270, Pakistan.

[n]Also at Ecole Polytechnique Federale de Lausanne (EPFL), CH-1015 Lausanne, Switzerland.

[o]Also at Helmholtz Institute Mainz, Staudinger Weg 18, D-55099 Mainz, Germany.